Biochimica et Biophysica Acta 1823 (2012) 1731–1744

Contents lists available at SciVerse ScienceDirect

Biochimica et Biophysica Acta

journal homepage: www.elsevier.com/locate/bbamcr

Connexin 43 phosphorylation and degradation are required for adipogenesis

Azadeh Yeganeh [a,c,f], Gerald L. Stelmack [c], Robert R. Fandrich [c,e], Andrew J. Halayko [c,d], Elissavet Kardami [b,c,e], Peter Zahradka [a,c,f,*]

[a] Department of Human Nutritional Sciences, University of Manitoba, Winnipeg, Canada
[b] Department of Human Anatomy & Cell Science, University of Manitoba, Winnipeg, Canada
[c] Department of Physiology, University of Manitoba, Winnipeg, Canada
[d] Department of Internal Medicine, University of Manitoba, Winnipeg, Canada
[e] Institute of Cardiovascular Sciences, St. Boniface Hospital Research Centre, Winnipeg, Canada
[f] Canadian Centre for Agri-food Research in Health and Medicine, St. Boniface Hospital Research Centre, Winnipeg, Canada

ARTICLE INFO

Article history:
Received 6 January 2012
Received in revised form 6 June 2012
Accepted 7 June 2012
Available online 15 June 2012

Keywords:
Adipogenesis
Connexin-43
Gap junction

ABSTRACT

Connexin-43 (Cx43) is a membrane phosphoprotein that mediates direct inter-cellular communication by forming gap junctions. In this way Cx43 can influence gene expression, differentiation and growth. Its role in adipogenesis, however, is poorly understood. In this study, we established that Cx43 becomes highly phosphorylated in early adipocyte differentiation and translocates to the plasma membrane from the endoplasmic reticulum. As preadipocytes differentiate, Cx43 phosphorylation declines, the protein is displaced from the plasma membrane, and total cellular levels are reduced via proteosomal degradation. Notably, we show that inhibiting Cx43 degradation or constitutively over-expressing Cx43 blocks adipocyte differentiation. These data reveal that transient activation of Cx43 via phosphorylation followed by its degradation is vital for preadipocyte differentiation and maturation of functional adipocytes.

1. Introduction

Gap junctions mediate intercellular communication by coordinating the transfer between adjacent cells of molecules less than 1000 Da in size, such as ions, amino acids, nucleotides, second messengers (e.g., Ca^{2+}, cAMP, cGMP, IP3), and various metabolites [1–3]. Various stimuli are responsible for gating these channels, including voltage changes, pH and phosphorylation [1–4].

Gap junction formation begins when six connexin proteins oligomerize into a hexameric hemi-channel, or connexon, in the endoplasmic reticulum. This complex is then transported through the Golgi and exported to the plasma membrane, where hemi-channels are available for gap junction assembly [5]. Formation of gap junctions occurs when a connexon from one cell pairs with a connexon from an adjacent cell [6,7].

An association between gap junction communication (GJC) and the differentiation of myoblasts and osteoblasts has been reported by several groups [8–11]. Inhibition of GJC by 18-α-glycyrrhetinic acid (AGA), a nontoxic reversible inhibitor of GJC, interfered with the progression of pre-osteoblastic MC3T3-E1 cells to an osteoblastic phenotype [10]. Likewise, Balogh et al. [8] reported that expression of Cx43, an abundant connexin that is expressed in most tissues, decreased during the differentiation of L6 skeletal myoblasts. Concomitantly, the GJC activity characteristic of myoblasts disappeared as myogenesis progressed.

Adipocytes are derived from the same progenitor cell as myoblasts and osteoblasts, however, the possibility that connexins have a similar role in adipocyte differentiation has not been investigated. Adipogenesis consists of two distinct phases: determination (or commitment) and terminal differentiation. Determination involves the commitment of a pluripotent stem cell to the adipocyte lineage, which results in conversion of the stem cell to a preadipocyte. In the second phase, terminal differentiation, the pre-adipocyte differentiates into a mature adipocyte and displays the characteristics associated with lipid transport and synthesis, the ability to respond to insulin and the production of adipokines. Current understanding of the molecular regulation of terminal differentiation has largely been attained using cell lines such as 3T3-L1 cells that are already committed to the adipogenic lineage. Differentiation of 3T3-L1 cells occurs in four stages: pre-confluent proliferation, confluence, mitotic clonal expansion and terminal differentiation [12]. The cells are made permissive for differentiation by maintaining them in a confluent state for 2 days, and adipogenesis is then induced by addition of an adipogenic and mitogenic cocktail containing dexamethasone, insulin and methylisobutylxanthine [13]. Hormonal induction leads to mitotic clonal expansion whereby cells undergo one or two rounds of mitosis over a 2 day period before terminally differentiating. Over the subsequent 4 days, the morphology of the cells changes from fibroblastic to spherical. In parallel, the cells accumulate lipid droplets and secrete adipokines.

* Corresponding author at: St. Boniface Hospital Research Centre, 351 Tache Avenue, Winnipeg, MB, Canada R2H 2A6. Tel.: +1 204 235 3507; fax: +1 204 237 4018.
E-mail address: peterz@sbrc.ca (P. Zahradka).

0167-4889/$ – see front matter © 2012 Elsevier B.V. All rights reserved.
doi:10.1016/j.bbamcr.2012.06.009

Azarnia and Russell [14] first reported that 3T3-L1 cells lose their ability to communicate via gap junctions as they differentiate. Umezawa and Hata [15] subsequently showed that expression of Cx43 is down-regulated at the transcriptional level during adipogenesis in H-1/A cells, a marrow stromal cell line that differentiates into adipocytes. More recently, Yanagiya et al. [16] reported that functional gap junctions are required for progression through a specific early stage of the 3T3-L1 preadipocyte differentiation program. However, there is currently no information regarding the role of Cx43 during the later stages of adipogenesis, particularly adipocyte maturation. Furthermore, the primary mechanisms that determine Cx43 subcellular location and phosphorylation state, as well as modulate Cx43-associated intercellular communication in the context of adipogenesis, have not been investigated.

Studies in other cell systems have shown that at least five different kinases target 12 or more serine and tyrosine residues within the regulatory C-terminal region of Cx43, including Src kinase, casein kinase 1 and p34cdc2. In addition, phosphorylation of Cx43 by mitogen activated protein kinase (MAPK) and protein kinase C (PKC) is required to close the hemichannels [17]. Another kinase that targets the Cx43 C-terminus is protein kinase A (PKA), which is activated by cyclic adenosine monophosphate (cAMP), one of the small molecules that can pass through gap junctions. In addition, Dowling-Wariner et al. [18] showed that Cx43 phosphorylation is necessary for differentiation of a human neural-glial cell line (SVG). They showed that treatment of SVG with PKA activators, such as forskolin or forskolin + 3-isobutyl-1-methylxanthine (MIX), can induce Cx43 phosphorylation along with SVG differentiation.

Given these strong associations between Cx43 and cell differentiation, we investigated for the first time both Cx43 localization and phosphorylation during 3T3-L1 adipogenesis. In addition, since the level of Cx43 decreases as adipocytes mature, we examined the role of proteasome activity in regulating Cx43 levels and the effects of constitutive Cx43 expression on adipocyte differentiation.

2. Materials and methods

2.1. Cell culture and treatments

3T3-L1 cells purchased from ATCC and 3T3-L1 CARΔ [19] generously provided by David Orlicky (Department of Pathology, University of Colorado Health Sciences Center, Denver) were grown in DMEM (Dulbecco's modified Eagle's medium). For 3T3-L1, 10% calf serum was added to the medium in the growth stage and 10% FBS (fetal bovine serum) during differentiation. In contrast, 10% HI-FBS (heat-inactivated FBS) was used for 3T3-L1 CARΔ in both growing and differentiating stages. The media were also supplemented with 20 mM HEPES, 100 units/ml penicillin and 100 μg/ml streptomycin. To induce differentiation, the cells were allowed to reach confluence and, after 2 days, cells were placed into DMEM (10% FBS or 10% HI-FBS) supplemented with 0.5 mM methylisobutylxanthine (MIX), 0.25 μM dexamethasone (DEX) and 10 μg/ml insulin (INS). This was considered day 0. After 2 days, the media were refreshed, but only 10 μg/ml insulin was added. The media were refreshed every 48 hours until the end of the experiment. Cells started differentiating on day 4. The cells could be cultured up to day 12, although most experiments were terminated by day 8.

2.2. Adenovirus infection

Adenovirus expressing Cx43 (Ad5.CMV.hCx43, Q Biogene) were titrated using the tissue culture infectious dose (TCID) method (Adeno-Quest™, Application Manual, Version 24AL98, Quantum Biotechnologies INC. Montreal, Canada). The Cx43-expressing adenovirus was applied to the 3T3-L1 CARΔ cells on day 0 (growth-arrested stage) at the same time as the adipogenic cocktail. Control adenovirus expressing GFP (Green Fluorescent Protein) (pAdeasy1/pshuttle CMV-EGFP) were kindly provided by Dr. Jeffrey Wigle (University of Manitoba). Expression of Cx43 was used to determine the efficiency of infection. Twenty-five MOI (multiples of infectivity) were employed in all experiments, since this was the most effective dose and produced the least cell death.

2.3. Western blot analysis

Protein was extracted from 3T3-L1 and 3T3-L1 CARΔ cells at various stages of differentiation by lysing with 2× sodium dodecyl sulfate (SDS) sample buffer. The samples were briefly sonicated to reduce viscosity and 10 μg of lysate protein was applied to SDS-polyacrylamide gels, transferred electrophoretically to PVDF (polyvinylidene difluoride) membranes and subsequently immunoblotted as described previously [20]. All horseradish peroxidase (HRP) conjugated secondary antibodies were used at a dilution of 1:10000 in TBST containing 1% BSA except rabbit HRP, which was used at 1:15000 (only for the total Cx43 polyclonal antibody). The primary antibodies employed in this study include rabbit anti-ACRP30 (adiponectin) (1:1000, Calbiochem), mouse anti-smooth muscle alpha actin (1:1000, Sigma), rabbit anti-Cx43 total (1:20000 [21]), rabbit anti-eEF2 (1:1000, Cell Signaling), mouse anti-fatty acid synthase (FAS) (1:1000, BD Transduction Laboratory), GAPDH (1:5000, Abcam), mouse anti-Oct-1 (1:500, Upstate) and anti-IGF-1 receptor β (1:1000, Cell Signaling). The relative band intensities were quantified by scanning densitometry with a model GS-800 Imaging Densitometer (Bio-Rad Laboratories, Hercules, CA).

2.4. Immunofluorescence microscopy

3T3-L1 or 3T3-L1 CARΔ cells were grown on coverslips and immunofluorescence microscopy was conducted as previously described [22]. Briefly, cells were fixed with fresh 4% paraformaldehyde, permeabilized with 0.1% Triton X-100 in PBS and after blocking with BSA were incubated overnight at 4 °C in a moist chamber with the primary antibody. This was followed by the secondary antibodies fluorescein-tagged donkey anti-rabbit Alexa 488 (1:500, Invitrogen) and Texas Red-conjugated donkey anti-mouse (1:250, Jackson Lab), and Hoechst 33342 (diluted 1:40000 in PBS). The coverslips were subsequently mounted (Bi∅Meda Corp.) and allowed to dry overnight. Negative controls lacking primary antibody were processed similarly. The cells were viewed and photographed using a Zeiss Axiovert 3.0 microscope. Axiovision Rel. 4.7 software was used to manipulate the captured images. The primary antibodies used were anti-ACRP30 (1:400), mouse anti-smooth muscle alpha actin (1:400), mouse anti-β-catenin (1:250, Santa Cruz), rabbit anti-calnexin (1:150, Cell Signaling), goat anti-calreticulin (1:400, kindly provided by Dr. N. Mesaeli [23]), rabbit anti-Cx43 total (1:2000), mouse anti-Cx43 total (1:100, Transduction Laboratory), mouse anti-unphosphorylated Cx43 (1:200, Zymed), mouse anti-FAS (1:250) and mouse anti-GM130 (1:250, Santa Cruz).

2.5. Subcellular fractionation

Cytosolic, membrane/cytoskeletal and nuclear fractions of 3T3-L1 cells were obtained with the subcellular Proteome Extraction kit (Calbiochem). Whole cell lysates were also collected for each condition. Western blotting (5 μg protein) was used to examine Cx43 content of each fraction in relation to specific marker proteins.

2.6. Laser scanning cytometry

The degree of association of Cx43 immunofluorescence in individual adipocytes that express FAS was measured using an iCys research imaging (laser scanning) cytometer (Compucyte Corp., Boston, MA, USA). Cells grown on cover slips were fixed, stained and mounted to glass slides as described under *Immunofluorescence microscopy*.

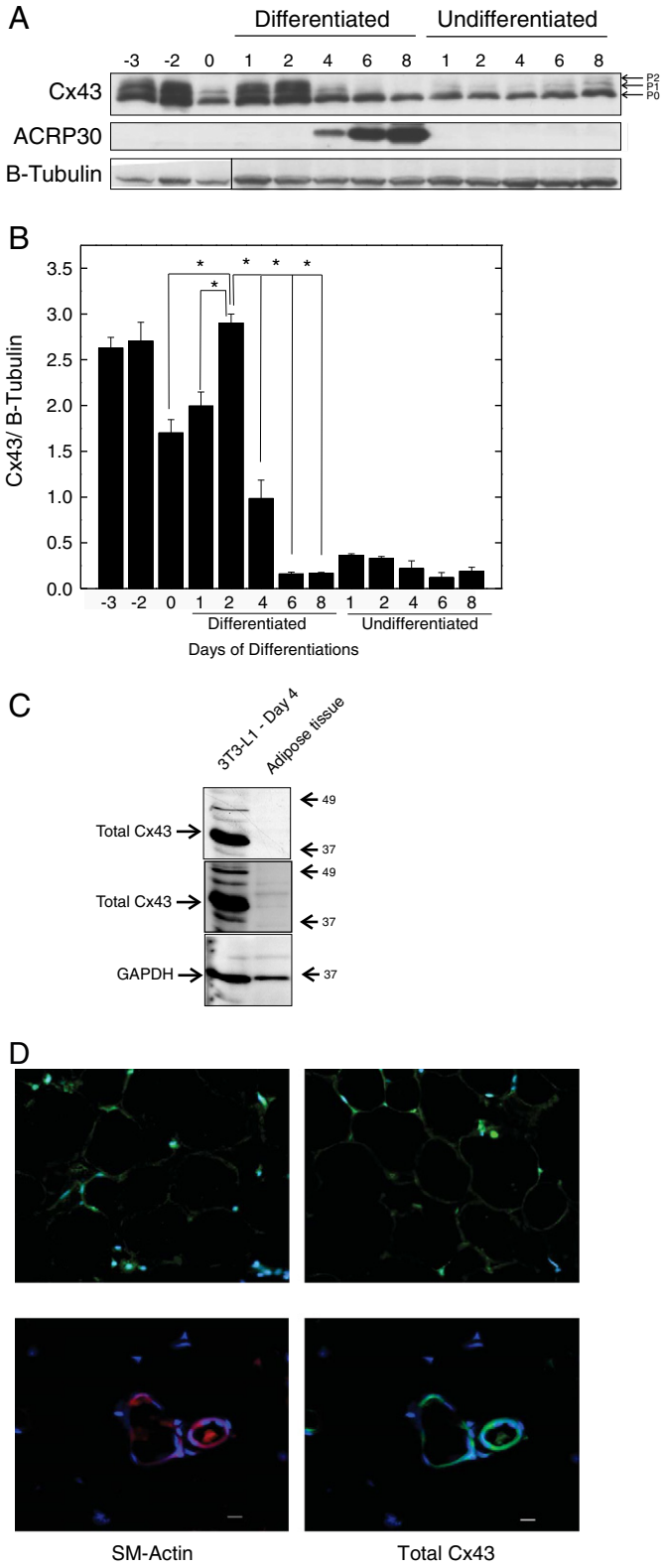

Fig. 1. Expression of Cx43 and its phosphorylated form during 3T3-L1 cell differentiation and in adipose tissue. (A) Levels of total Cx43, ACRP30 (adipocyte marker) and eEF2 (loading control) in lysates prepared from 3T3-L1 cells undergoing adipogenesis were determined by Western blotting. Day 0 represents the undifferentiated preadipocyte and day 8 is the mature adipocyte. A representative gel is shown. (B) Total Cx43 band intensity was quantified by scanning densitometry ($n = 4$). Data were normalized to the loading control (eEF2). Mean ± SEM is shown (*$P < 0.05$). (C) Representative Western blot of adipose tissue probed for total Cx43. Cell lysate of 4 day differentiated 3T3-L1 cells was used as a positive control. GAPDH served as loading control. (D) Immunofluorescence staining of 5 μm sections of rat adipose tissue for total Cx43. No difference was observed between control (top right panel, without primary antibody) and the actual experiment (top left panel, with primary antibody). Total Cx43 is indicated in green and nuclei are stained blue. The bottom panels show sections of rat adipose tissue stained for vascular smooth muscle with smooth muscle α-actin (red, left) and Cx43 (right, green). Cx43 is present in the blood vessel but not in adipocytes. Bar, 10 μm. Images were captured using a 40× objective.

After primary antibody incubations, immunoreactive punctae of Cx43 and FAS expressing cells were labeled with Alexa 488- and Cy3-conjugated secondary antibodies, respectively. Cell nuclei were stained directly with Hoescht 33342. For imaging, excitation of the chromophores was achieved with 405 nm (nuclei and Cx43) and 488 nm (FAS) laser lines. Emission was measured at 463 ± 39 nm (blue channel, nuclei); 530 ± 30 nm (green channel, Cx43) and 580 ± 30 nm (red channel, FAS).

Fluorescent imaging and quantitative fluorescence measurements were collected from multiple scan fields (200 × 192 μm; pixel resolution of 0.2 × 0.25 μm) on each sample, with cumulative scan areas from 3.4 to 7 mm^2. For all analyses total fluorescence was integrated within the boundaries of regions of interest (contours) that were generated as described hereafter. iCys software parameters for green channel (Cx43) fluorescence were quantified in a signal-dependant manner to generate primary contours (regions of interest) that associated specifically with the punctate immunofluorescence pattern for Cx43 in individual cells. Red channel fluorescence (FAS) was quantified using a "Phantom contour" protocol in which 8 μm diameter circular contours (phantoms) were arranged as a non-overlapping lattice over the

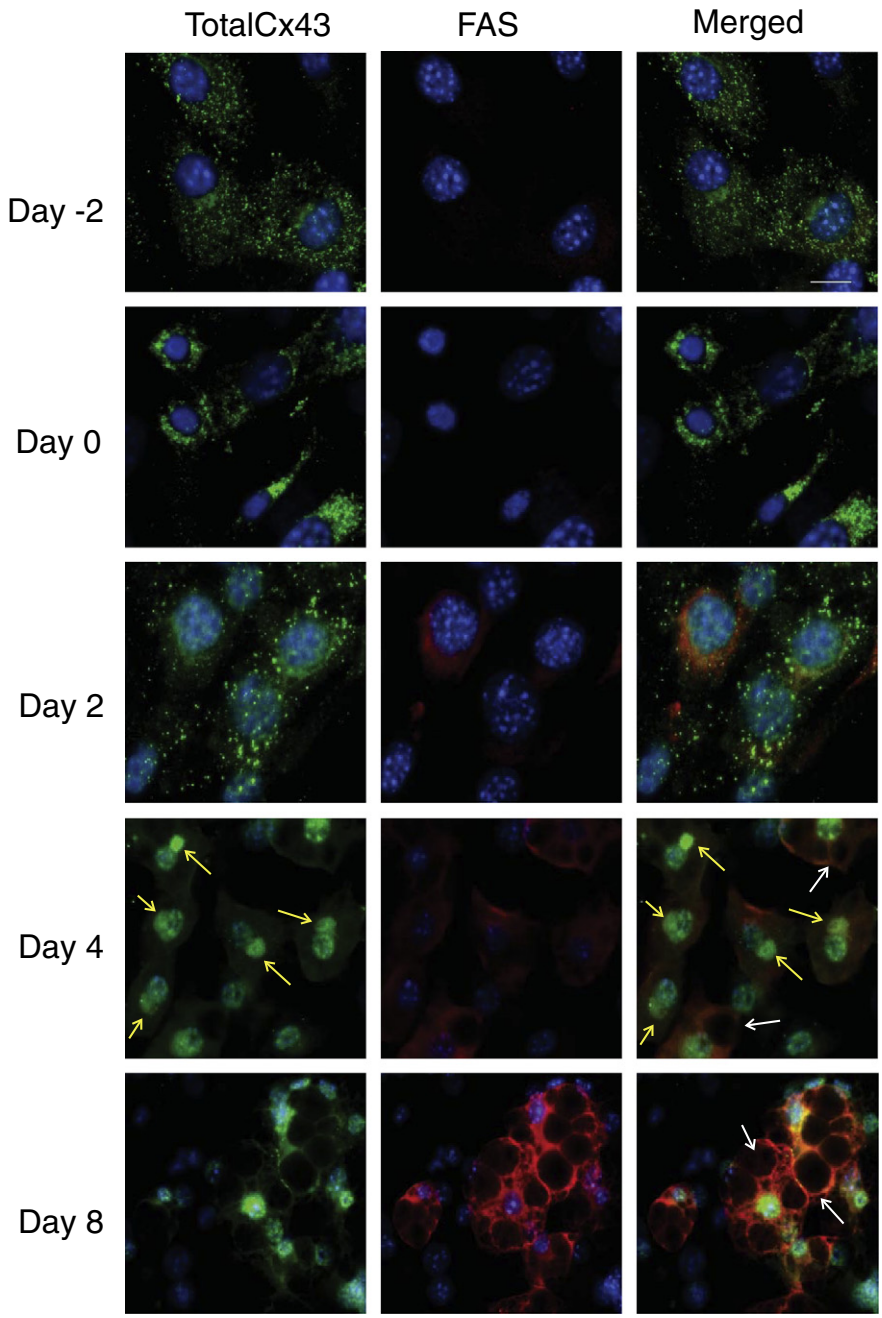

Fig. 2. Phosphorylation and localization of Cx43 in the early stages of adipocyte differentiation. Immunofluorescence staining was performed on fixed cells at different stages of differentiation as indicated on the left. The photos depict cells on day −3/−2 (growing), day 0 (growth arrested), day 2 (mitotic clonal expansion), day 4 (mid-differentiation), day 6 or 8 (differentiated). The pictures are representative of 3 independent experiments. (A) Total Cx43 is indicated in green, FAS in red and the nuclei are blue. The white arrows show the lipid droplets in differentiated cells on days 4 and 8 and the yellow arrows point to perinuclear Cx43 staining on day 4. (B) The cells were co-stained with total Cx43 and unphosphorylated Cx43 antibodies and images of these individual antibodies were merged to identify phosphorylated Cx43. Green is total Cx43 and red is unphosphorylated Cx43. Arrows (day −3 merged) show the location of phosphorylated Cx43 (yellow). Bar, 2 μm (indicated on day −23 merged image), is applicable to all panels. Images were captured using a 40× objective.

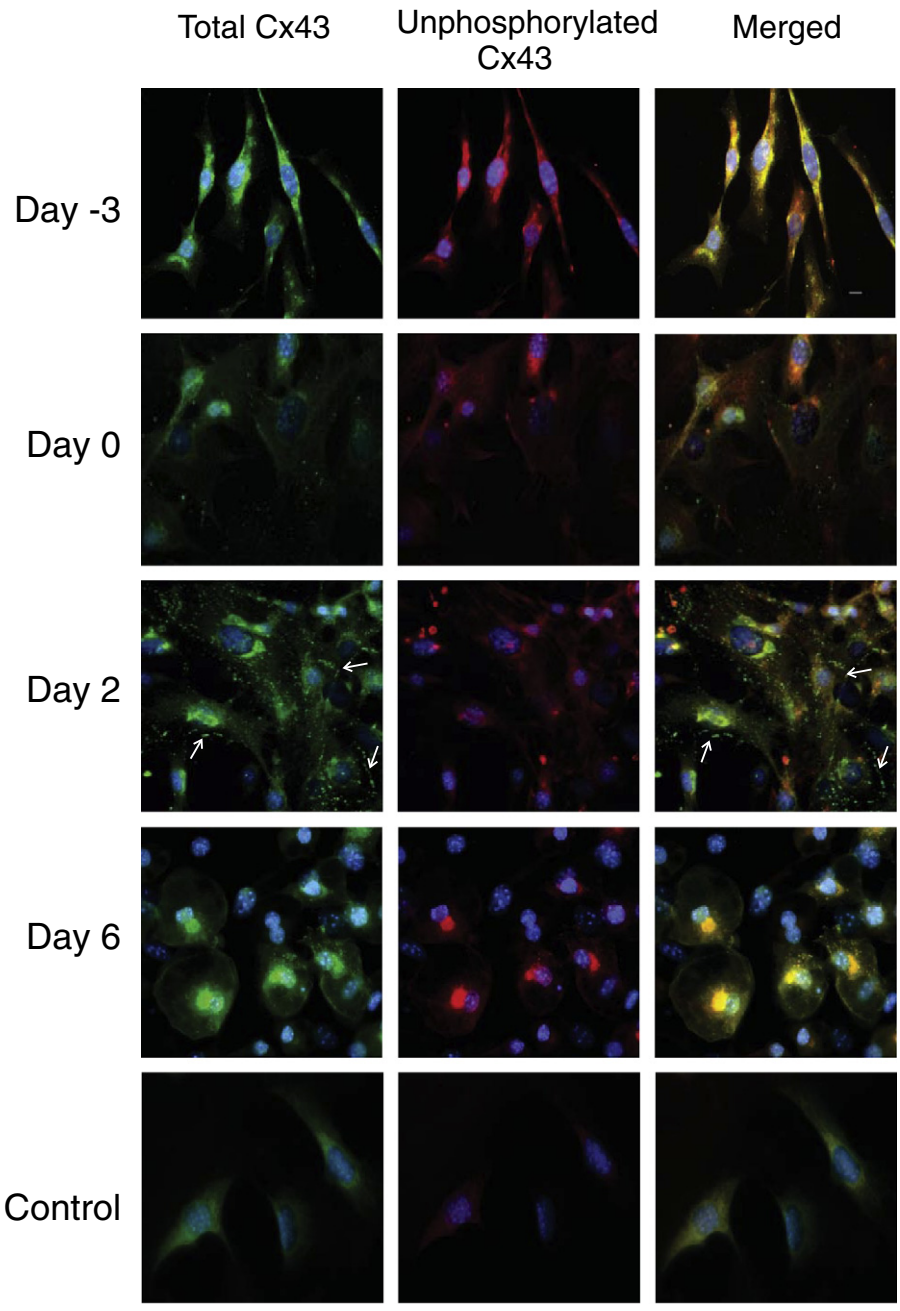

Fig. 2 (*continued*).

whole scan area, allowing for the quantification of Cy3 fluorescence within the scan area at regularly spaced coordinates. Spatial overlap of individual primary (Cx43) and phantom contours (FAS) was determined using iCys software. Threshold fluorescence for regions of "high" or "low/negative" FAS (red) fluorescence, respectively, were identified from frequency histograms of cells labeled with or without (primary omission) primary antibody included.

2.7. Statistical analysis

Data are presented as mean ± SEM (standard error of the mean). Statistical analysis was performed using one way analysis of variance (ANOVA) using SAS program (SAS Institute Inc, NC, USA), as indicated in the figure legends. All experiments were independently repeated at least 3 times. Significant differences among group means were determined with Duncan's Multiple Range test. Differences were considered statistically significant at $P<0.05$.

3. Results

3.1. Expression of Cx43 during 3T3-L1 differentiation and in adipose tissue

To examine the expression of total Cx43 during adipogenesis, 3T3-L1 cells were differentiated as described under Materials and methods via addition of an adipogenic cocktail containing INS, DEX and MIX to cells that had been confluent for 2 days [15]. Progression of 3T3-L1 differentiation involves passage over a period of 8 days through four distinct stages, pre-confluent proliferation, confluence, mitotic clonal expansion and terminal differentiation [14], which can be distinguished by monitoring cell morphology, accumulation

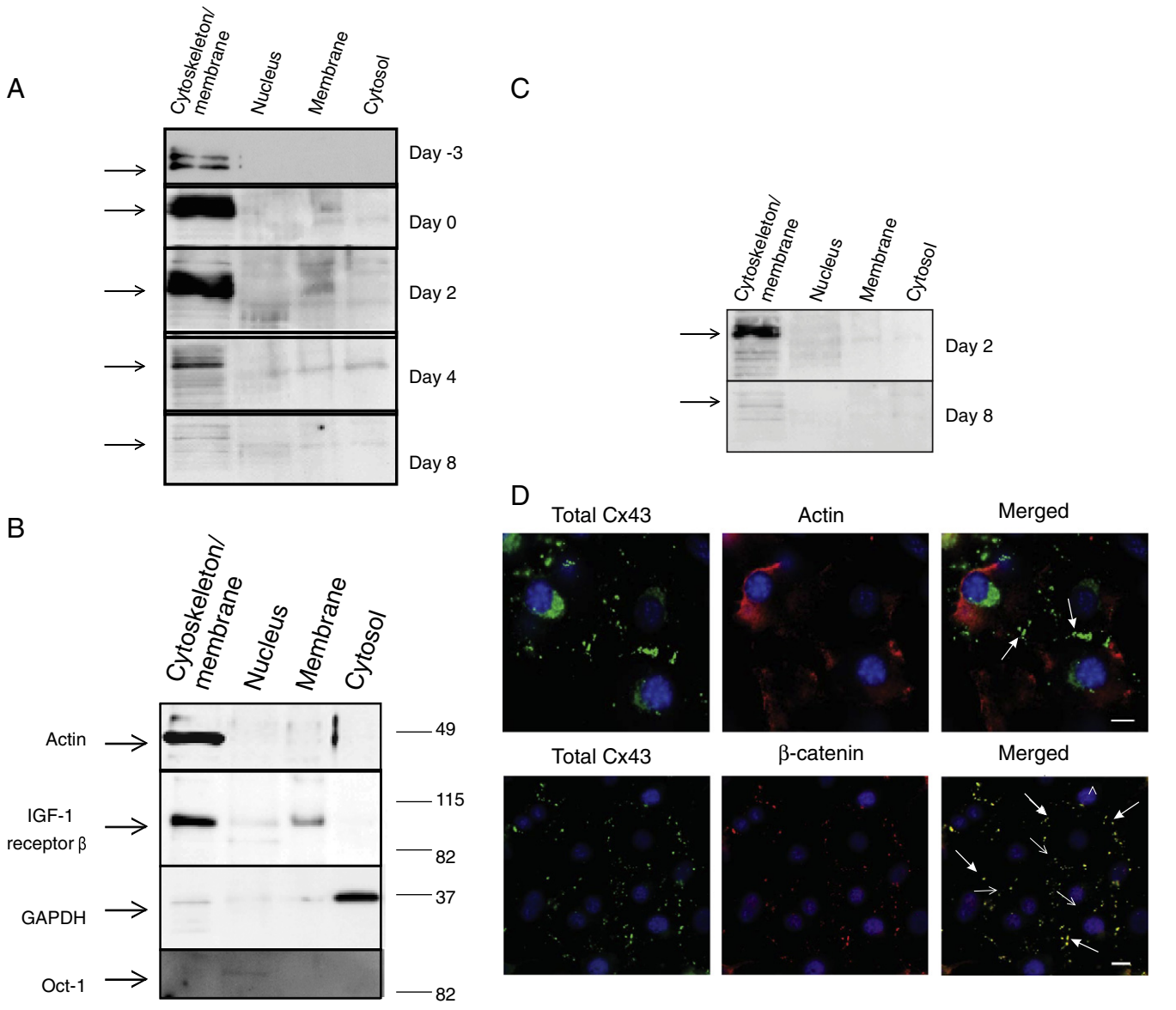

Fig. 3. Subcellular fractionation of 3T3-L1 cells during adipogenesis. (A) Representative Western blot of subcellular fractions obtained from 3T3-L1 cells on day −3 (growing), day 0 (growth arrest), day 2 (mitotic clonal expansion), day 4 (mid-differentiation) and day 8 (fully differentiated) for total Cx43. (B) Western blot of 3T3-L1 cell fractions, probed with different markers for each fraction. α actin = cytoskeleton, IGF-1 receptor β = membrane, GAPDH = cytosol and OCT-1 = nucleus. (C) Western blot of undifferentiated 3T3-L1 fractions on days 2 and 8, probed for total Cx43. (D) 3T3-L1 cells were fixed on day 2 and subsequently examined by immunofluorescence microscopy for total Cx43 (green) and either β-catenin or α-actin (red). Areas of overlap between β-catenin/α-actin with Cx43 are indicated by the arrow 2 on the merged pictures. Bar, 10 μm (indicated on merged images), is applicable to all panels. Images were captured using a 40× objective.

of lipid droplets and secretion of adipokines. The Cx43 content from days −3 to 8 was determined by Western blotting with an antibody that detects both phosphorylated and unphosphorylated Cx43 (Fig. 1A, B). Cx43 displays an apparent electrophoretic mobility at 41–45 kDa, with non-phosphorylated (or minimally phosphorylated) Cx43 at 41 kDa (P0), and increasingly phosphorylated Cx43 at >41 kDa (P1, P2). Preadipocytes on days −3 and −2 have high levels of total Cx43 (both P0 and P1-P2 bands) and the levels decreased slightly by day 0 (2 days post-confluence). In contrast, the amount and phosphorylation of Cx43 was markedly increased in adipocytes 2 days after triggering differentiation ($P=0.001$, $n=5$) (Fig. 1A, B). Subsequently, levels of total as well as P1–P2 Cx43 decreased as adipocyte differentiation proceeded and by day 4 (early differentiation) P1–P2 Cx43 were no longer detectable. Likewise, P0 Cx43 also decreased compared to day 2 ($P=0.001$, $n=5$), however, it likely remained detectable in day 8 cultures due to the presence of preadipocytes, since 10–20% of these cells typically do not differentiate [24]. In these experiments, we used ACRP30 as a marker for adipocyte maturation; its expression was first detected in 3T3-L1 cells on day 2 (completion of mitotic clonal expansion) and was maximally expressed from early-differentiation (day 4) until the experiment was terminated when adipocytes were fully differentiated (Fig. 1A). Collectively, these data show that an increase in Cx43 and its phosphorylation precedes adipocyte differentiation and these are down-regulated as adipogenesis proceeds. In parallel, the same experiment was done with undifferentiated cells, and these data showed that there was no increase in Cx43 after day 0 (Fig. 1A, B). The lack of adiponectin indicated these cells had not differentiated (Fig. 1A).

To confirm that Cx43 abundance is in fact low in mature adipocytes *in situ*, we also examined total Cx43 in protein extracts prepared from the perirenal adipose tissue of 15-week-old male lean Zucker rats (kindly provided by Dr. C. Taylor, University of Manitoba). Cx43

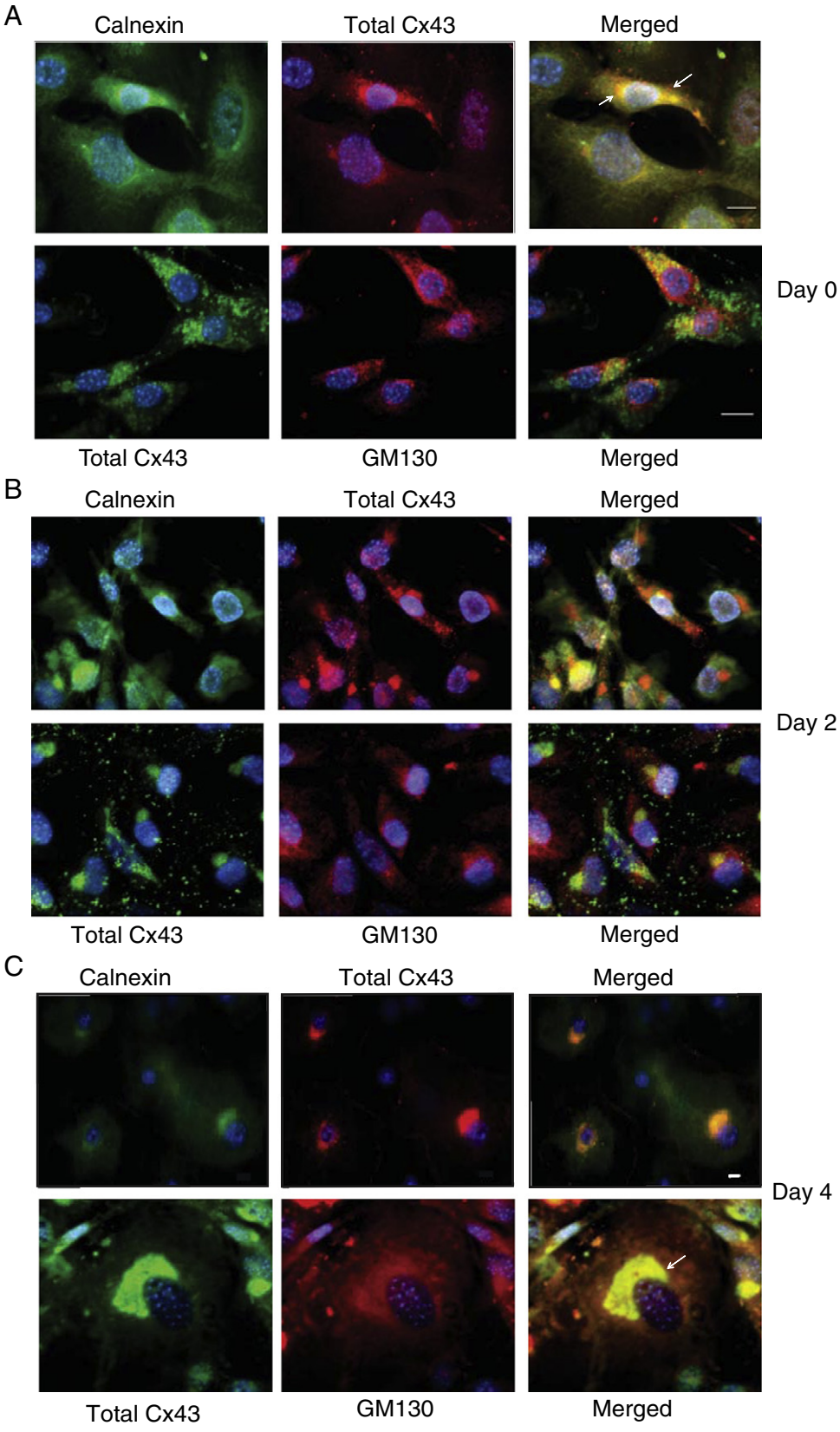

Fig. 4. Adipogenesis influences subcellular location of Cx43. 3T3-L1 cells were fixed on (A) day 0 (growth arrested), (B) day 2 (mitotic clonal expansion) and (C) day 4 (mid-differentiation) and subsequently co-stained with calnexin (ER marker, green, upper row) and total Cx43 (red, upper row), or co-stained with GM130 (Golgi marker, red, lower row) and total Cx43 (green, lower row). The last image on each panel is a merger of the first two images, with arrows showing areas of overlap between Cx43 and the ER and Golgi markers. The images are representative of the results obtained from two independent experiments. Bar, 2 μm (indicated on first merged image), is applicable to all panels. Images were captured using a 40× objective.

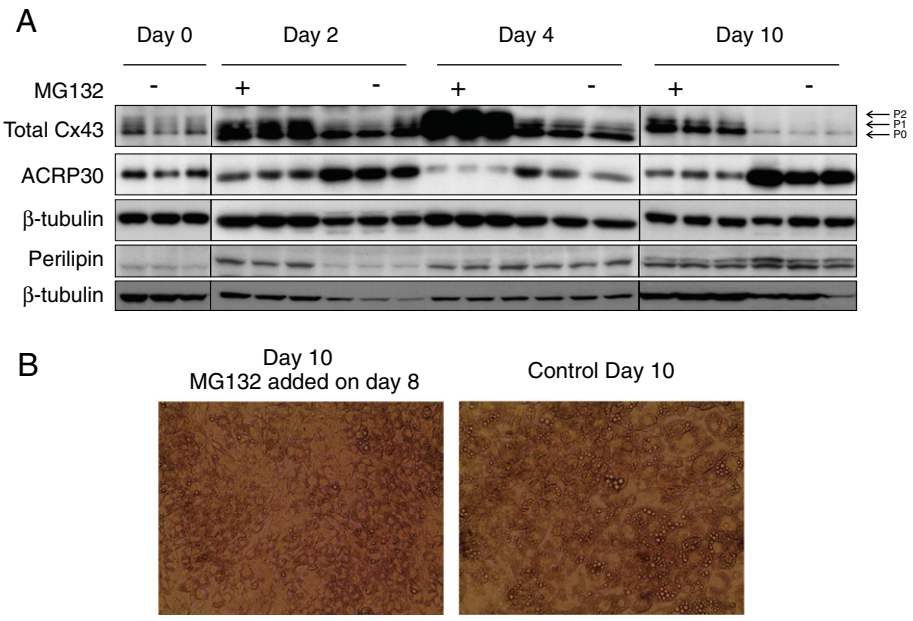

Fig. 5. Effect of MG132 on adipogenesis and Cx43 level and phosphorylation. 3T3-L1 cells were treated with 5 μM MG132 for 48 h (A) on days 0 2 and 8 of differentiation. The cells treated with MG132 on day 0 and lysed after 48 hours are designated day 2 samples. Likewise cells treated on day 2 and lysed on day 4 are day 4 samples, and mature adipocytes treated on day 8 and lysed on day 10 are day 10 samples. Western blotting shows the level of total Cx43, ACRP30 (adipocyte marker), perilipin (lipid droplet protein) and β-tubulin (loading control). Samples of day 2 and day 4 were run on the same gel and day 0 and day 10 samples were run on a different gel. The internal controls revealed the intensity of the bands on the different gel are reasonably comparable. The figure is representative of at least three independent experiments.

was not detectable in the tissue sample by Western blotting (a lysate of 3T3-L1 cells treated with adipogenic cocktail was used as a positive control). Although a longer exposure time revealed Cx43 was present, it is plausible that this low level of Cx43 is due to the presence of other cell types in adipose tissue that contain Cx43 (Fig. 1C). Furthermore, immunofluorescence labeling of perirenal adipose tissue sections for Cx43 antibody revealed the degree of staining was not different from the negative control (lacking primary antibody) (Fig. 1D). A section of adipose tissue that included a blood vessel was chosen as the positive control. Since vascular smooth muscle cells express both Cx43 and smooth muscle α-actin, dual staining of Cx43 and smooth muscle-actin was performed. The micrograph shows that Cx43 is present within vessels that are actin positive, but not in the adipocytes that are actin negative (Fig. 1D).

3.2. Expression and localization of Cx43 during adipogenesis

Immunocytochemistry was performed on 3T3-L1 cells undergoing adipogenesis. Specifically, cultures were assessed at multiple stages: preadipocytes (growing (day −2) and growth arrested (day 0)); mitotic clonal expansion (day 2); mid-differentiation (day 4); and fully differentiated (day 8). Cells were labeled for Cx43 and for FAS, with the latter used as a marker for mature adipocytes (Fig. 2A).

In preadipocytes (days −2 and 0), Cx43 was abundant and localized to punctate bodies that were most abundant near the nucleus on day 0 (Fig. 2A). In contrast, in cultures where cells were undergoing mitotic clonal expansion and FAS expression was visible in some cells (day 2), punctate Cx43 was found primarily on the periphery of the cells. A marked change in staining occurred as cells underwent differentiation and accumulated FAS; specifically, the punctate staining was lost and became relatively low. At mid-differentiation, coalesced patches of perinuclear Cx43 staining were visible (yellow arrows), but these were absent in fully differentiated adipocytes. These data reveal that, as preadipocytes mature into adipocytes, both the amount of Cx43 and its location in gap junctions (punctate staining pattern [22]) decreases (Fig. 2A). As the negative control shows, background staining in both the total Cx43 and FAS images could explain the presence of the light yellow color in the mature day 8 cells that express FAS. This experiment also confirmed that not all cells differentiate and that the low levels of Cx43 seen on day 8 (Fig. 1A) are due to the preadipocytes that remain.

To examine the phosphorylation status of Cx43 during adipogenesis, immunofluorescence staining was performed with a rabbit polyclonal anti-Cx43 antibody that detects total (phosphorylated and unphosphorylated) Cx43 and a mouse monoclonal antibody that detects only the unphosphorylated Cx43(P0). In our case, the green color represents total Cx43 (phosphorylated + unphosphorylated) while the red color is indicative of unphosphorylated Cx43. The yellow color therefore corresponds to phosphorylated Cx43. This distinction relates to the properties of the antibodies and the forms of Cx43 they recognize and is described in more detail in an earlier publication [22]. The unique properties of these antibodies make it necessary to use dual staining to localize the phosphorylated forms of Cx43 within the cell. Consequently, matched images of cells labeled with each individual antibody were merged, resulting in differential labeling of the unphosphorylated (yellow) and phosphorylated (green) Cx43. Our analyses show that preadipocytes contain both phosphorylated and unphosphorylated Cx43 (Fig. 2B), as yellow and green are both visible in the merged picture. Cx43 phosphorylation increased in the confluent cells (day 0) and during the mitotic clonal expansion phase (as observed in Fig. 1). In mature (day 6) adipocytes, however, Cx43 is only present in its unphosphorylated form as indicated by the absence of green, which represents Cx43 phosphorylation in the merged picture. These data establish that on day 2 of differentiation Cx43 becomes phosphorylated and localizes to the cell periphery, likely due to incorporation into gap junctions.

3.3. Subcellular localization of Cx43 during adipogenesis

Since the pattern of immunofluorescence staining suggests that Cx43 localization changes during adipocyte differentiation (Fig. 2A, B), we next used subcellular fractionation and immunoblotting to more clearly determine which cellular compartment(s) contained Cx43 at different stages of adipogenesis. Fractions of 3T3-L1 cells

were prepared from growing (day −3), growth arrested (day 0), mitotic clonal expansion (day 2), mid-differentiation (day 4) and differentiated (day 8) cells. To serve as non-differentiated controls, we also prepared cell fractions from post-confluent cultures maintained in growth media that was not supplemented with pro-adipogenic cocktail. These control cells were lysed either 2 or 8 days after their day 0 counterparts. Immunoblotting indicated that the total abundance of Cx43 was markedly reduced during differentiation. On the other hand, the relative subcellular localization of the protein remained more-or-less consistent, being principally enriched in cytoskeleton/membrane fractions characterized by high levels of IGF-1 receptor β (Fig. 3A and B). The same pattern was present in control undifferentiated 3T3-L1 cells (Fig. 3C).

Although the kit employed for subcellular fractionation was designed to separate the cytoskeletal fraction from the membrane fraction, we found cross-contamination between these fractions (the membrane marker, IGF-1 receptor β, was present in both fractions). For this reason, the cytoskeletal fraction was termed the cytoskeletal/membrane fraction in Fig. 3. To resolve this issue of membrane versus cytoskeletal localization, co-staining for total Cx43, α-actin (cytoskeleton marker) and β-catenin (plasma membrane marker) was performed using cells on day 0 or 2 of differentiation. In the merged images we observed no overlap between actin fibers and Cx43, thus indicating Cx43 was not associated with microfilaments (Fig. 3D). In contrast, Cx43 and β-catenin were overlapped, thus establishing that Cx43 is enriched in the plasma membrane fractions of these cells (Fig. 3D). However, in apparent contrast to these data are our immunocytochemistry analyses (Fig. 2A) that clearly show the distribution of Cx43 changes markedly with differentiation.

These paradoxical observations suggest that in addition to the plasma membrane Cx43 might also be associated with one or more membranous organelles, such as the Golgi apparatus or the endoplasmic reticulum (ER). To address this issue, 3T3-L1 cells were co-stained on day 0 (growth arrested), day 2 (mitotic clonal expansion) and day 4 (mid-differentiation) for Cx43 and specific markers of the Golgi (GM130) and ER (calnexin). On day 0, colocalization with calnexin established that Cx43 was localized to the ER, whereas the protein did not appear to be associated with GM130-labelled Golgi membranes (Fig. 4A). Notably, 2 days after adding adipogenic medium, when Cx43 abundance and phosphorylation was at its highest (Fig. 1A) and was enriched in the membrane fraction (Fig. 3A), we observed only weak staining of Cx43 in the Golgi and ER suggesting it was present predominantly in the plasma membrane (Fig. 4B). On day 4 (early differentiation), when Cx43 abundance and phosphorylation waned (Figs. 1A and 3A), staining for Cx43 in both the Golgi and ER compartments became more prominent again (Fig. 4C). On day 8, morphogenesis to a differentiated adipocyte replete with lipid droplets was associated with the abrogation of ER and Golgi-associated Cx43 staining (not shown).

3.4. Cx43 regulation during adipogenesis

To examine the contribution of the proteasome pathway to the disappearance of Cx43 in the latter stages of adipogenesis, 3T3-L1 cells were treated for 48 hours with 5 μM of MG132 (Z-Leu-Leu-Leu-CHO), a proteasome inhibitor. The compound was added at different times during differentiation: days 0, 2, 4, 6 and 8. Dose and time were assessed in pilot experiments to determine the optimum treatment conditions (not shown). Addition of MG132 to preadipocytes (days 0 and 2) for 48 hours resulted in an elevation of total Cx43 (both phosphorylated and unphosphorylated forms) (Fig. 5A). MG132 treatment concomitantly prevented the increase in proteins (adiponectin, perilipin) typically seen in mature adipocytes (Fig. 5A), which suggests this compound blocked adipogenesis. MG132 treatment of mature adipocyte (day 8) likewise caused an increase in total Cx43 (both phosphorylated and unphosphorylated forms), which closely resembled the pattern seen in growth-arrested preadipocytes (day 0) (Fig. 5A). In parallel, inhibition of proteoasome activity on day 8 caused a reduction in the level of adiponectin (Fig. 5A), indicative of a reversion towards the preadipocyte stage. Similar results were obtained with days 4 and 6 cells (data not shown). These data suggest that the reduction of Cx43 levels and Cx43 phosphorylation during differentiation after day 3 is necessary both for adipogenesis and for preserving the mature adipocyte phenotype. Although there are reports that indicate MG132 promotes cell death [25,26], the fact that the level of β-tubulin did not change makes this possibility unlikely in these experiments, and this conclusion was supported by the fact both cell number and cell morphology was unaffected after treatment for 48 hours with MG132 (Fig. 5B).

3.5. Effect of constitutive expression of Cx43 during adipogenesis

Since Cx43 decreased in cultures after the clonal expansion phase and our studies using a proteoasome inhibitor suggest Cx43 down-regulation is linked to adipocyte differentiation, we next investigated whether selective induction of Cx43 expression was sufficient to modulate adipogenesis. Adenoviral infection of 3T3-L1 cells is inefficient [27], thus we employed 3T3-L1 CARΔ cells that express a gene encoding the coxsackie and adenovirus receptor (CAR) [19], a modification that imparts much improved adenovirus infection efficiency relative to 3T3-L1 cells. Preliminary experiments in which Ad. CMV-hCx43 adenovirus was applied at 0, 25, 50 and 100 MOI established that 25 MOI provided the greatest expression of Cx43 without causing cell death (data not shown).

Two-day post-confluent 3T3-L1 CARΔ cells (day 0) were treated with adipogenic medium and concurrently infected with Ad5.CMV-hCx43. Controls were treated with the same cocktail and infected with GFP adenovirus. The experiment was terminated by addition of lysis buffer to cells on days 0, 2, 4 and 8, and differentiation was quantified by immunoblotting for adiponectin. Day −2 cells were used as a growing stage control in this experiment. Infection with Ad5.CMV-hCx43 increased the Cx43 content of the cells within 2 days, reaching a maximum within 4 days and remaining elevated for the 8-day duration of the experiment (Fig. 6A). While 37% of the cell population expressed higher amounts of Cx43 (measured by counting cells stained for total Cx43 on 4 different fields, repeated on 4 separate occasions), immunoblotting was unable to detect a significant change in adipokine production in the cultures as a whole (Fig. 6A). Moreover, it was not possible to use a higher MOI of Ad5.CMV-hCx43 to increase infection efficiency (which was 37%) as cell toxicity became excessive (this is a characteristic of adenoviral treatment also seen with skeletal myoblasts [28]). Therefore, to overcome the limitations of using Western blotting to assess potential changes in expression in only a sub-population of the cells, we next employed immunofluorescence labeling to examine the expression of differentiation markers on a cell-by-cell basis after Ad5.CMV-hCx43 infection. This analysis specifically used cells that had been maintained for 8 days in differentiation medium (i.e. 8 days after adenovirus infection). Foci of Cx43 immunolabelling were localized to the periphery of the infected cells and non-punctate staining was also evident, appearing to be present in the cytoplasm (Fig. 6B). Unlike GFP infected cells, which expressed GFP in differentiated cells that contained lipid droplets (Fig. 6C), visual inspection of Ad5 CMV-Cx43 infected cells showed that the cells expressing Cx43 did not express FAS and did not contain lipid droplets (Fig. 6D). To confirm these visual observations, the total number of Ad5 CMV-Cx43 infected and FAS expressing cells were counted on 3 different $200 \times 192\ \mu m^2$ fields (Fig. 6E). This approach revealed that among the Ad5 CMV-Cx43 infected cells only $1.6 \pm 0.3\%$ expressed FAS and none contained lipid droplets.

To objectively quantify the immunofluorescence data, we employed laser scanning cytometry (LSC) of infected and wild type cells on day 8. LSC analysis enabled identification of individual Cx43

punctae (Fig. 7A, B, D, E) in uninfected and Cx43-adenovirus infected 3T3-L1 CARΔ. In addition, by overlaying a matrix of phantom contours using CompuCyte LSC software (see Materials and methods), individual cells in which FAS was present (FAS +'ve) and absent (FAS –'ve) could be discriminated (Fig. 7C, F). We first used LSC to determine the impact of Ad5 CMV-Cx43 infection on the number of Cx43 punctae in individual cultures, and found infection led to a 2.8-fold increase compared to wild type 3T3-L1 CARΔ cells (Fig. 7G). Frequency distribution data for FAS positive and FAS negative regions were determined and plotted as a histogram for both wild type uninfected and Ad5 CMV-Cx43 infected 3T3-L1 CARΔ cells (Fig. 7H). We next assessed the frequency association of Cx43 punctae with cellular regions of FAS staining (Fig. 7H). Frequency histograms clearly show that Cx43 events associate readily with FAS negative regions, whereas Cx43 punctae are 75–85% less frequent in regions where positive labeling for FAS was obtained (Fig. 7I). This frequency association was a characteristic of both wild type and Ad5 CMV-Cx43 infected 3T3-L1 CARΔ cultures. Collectively, these data confirm the findings of Fig. 6 and demonstrate that expression of FAS in individual cells is inversely correlated with the presence of Cx43 punctae.

4. Discussion

This investigation is the first to report that failure to reduce Cx43 levels after the mitotic clonal expansion stage blocks differentiation of preadipocytes, thus establishing that Cx43 degradation is essential for adipogenesis. This conclusion is based upon data obtained using a proteasome inhibitor as well as by constitutively expressing Cx43 via adenoviral infection. Furthermore, the Cx43 levels and subcellular distribution closely correlated with phosphorylation state. As a result, we propose that Cx43 has two critical functions: 1) making preadipocytes permissive for differentiation, and 2) enabling adipocyte maturation.

We have demonstrated that Cx43 expression undergoes major changes during adipogenic differentiation: its expression was robustly increased 2 days after addition of the adipogenic cocktail during clonal induction and, as reported by others [16], Cx43 levels decreased as 3T3-L1 cells differentiated into mature adipocytes. In agreement with our cell culture data, we showed that Cx43 is not detectable in adipose tissue. During clonal induction, Cx43 is in a highly phosphorylated state (indicated by bands at P1-P2) and this is likely associated with an increase in gap junction communication [14]. Subsequently, as adipocytes start to differentiate, a process that can be recognized by morphological changes and lipid droplet accumulation, Cx43 abundance is markedly reduced. A decrease in relative levels of P1-P2 Cx43 precedes the decline in total Cx43, and is closely coupled to changes in its subcellular compartmentalization (Fig. 4). Cx43 migrated from the endoplasmic reticulum in preadipocytes to the plasma membrane of cells in the early stages of differentiation, likely in response to changes in its phosphorylation as indicated by a relative

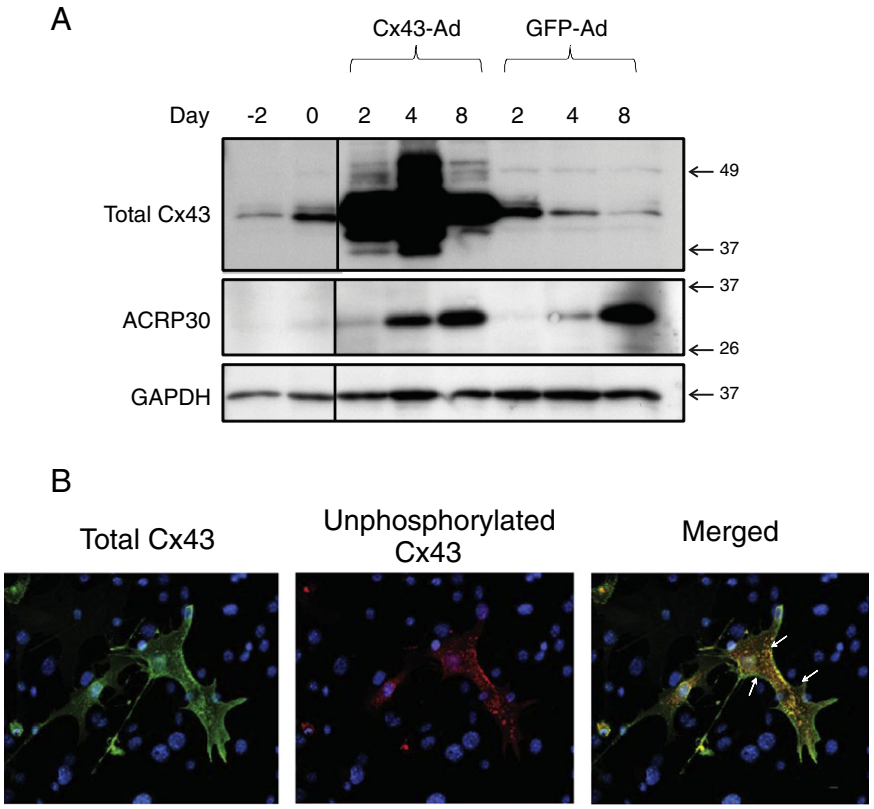

Fig. 6. Effect of constitutive expression of Cx43 on 3T3-L1-CARΔ differentiation. (A) 3T3-L1-CARΔ cells were infected on day 0 with Ad5 CMV-Cx43, and Western blotting was used to monitor total Cx43 and ACRP30 levels on day −2 (preadipocytes), day 0 (growth arrested), day 2 (mitotic clonal expansion), day 4 (mid-differentiation) and day 8 (differentiated). Total Cx43 in GFP adenovirus infected 3T3-L1-CARΔ on days 2, 4 and 8 is also shown. GAPDH was used as the loading control. The figure is representative of 3 independent experiments (the bands from the uninfected cells were removed for clarity). (B) Cells infected with Ad5 CMV-Cx43 were co-stained for total Cx43 (green) and unphosphorylated Cx43 (red). Phosphorylated Cx43 was identified by merging the images. The arrows in the merged picture indicate the location of the phosphorylated form of Cx43 (green); the yellow color (overlap of green and red) represents the unphosphorylated form of Cx43; red is not visible because it overlaps completely with total Cx43. Bar, 2 μm (indicated on merged image). Images were captured using a 40× objective. **(C)** 3T3-L1-CARΔ cells were infected on day 0 with adenovirus carrying GFP. The cells were fixed on day 6 and immunostaining applied. Lipid droplets are visible in differentiated GFP positive cells. Red arrows signify GFP-negative spherical cells with lipid droplets and white arrows indicate GFP-positive cells. Bar, 40 μm. Images were captured using a 10× objective. (D) Total Cx43 (green) and FAS (red) in 3T3-L1 cultures 6 days after infection with Ad5 CMV-Cx43. (E) Number of cells expressing Cx43, Cx43 + FAS and Cx43 + lipid (LD) droplets 6 days after infection with Ad5 CMV-Cx43 was determined in 3 different 200 × 192 μm fields.

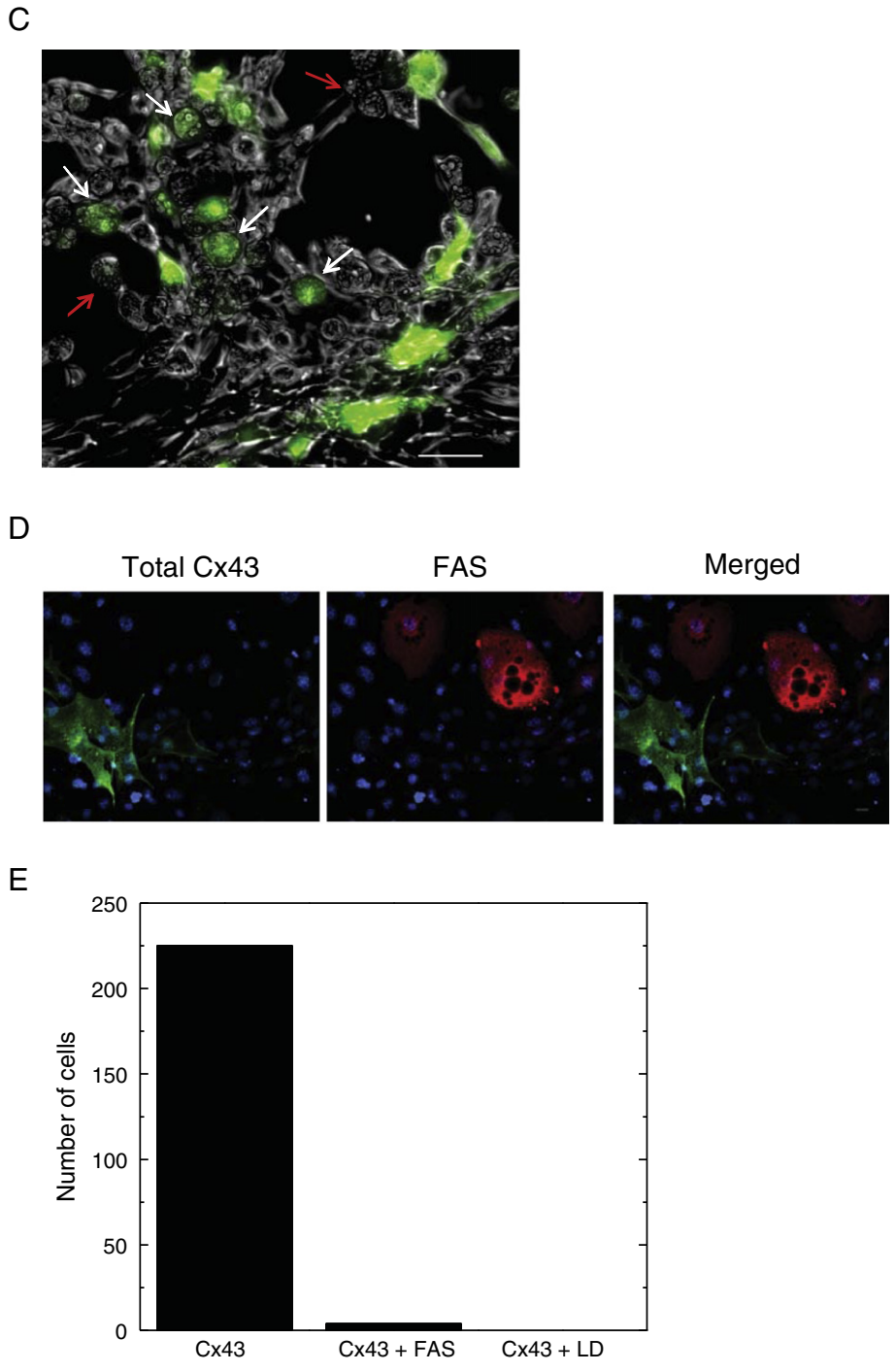

Fig. 6 (*continued*).

increase in P2. Subsequently, Cx43 relocates to the ER as the adipocytes mature and then undergoes proteasomal degradation. This change in subcellular location likely explains how functional gap junctions could be transiently generated during initiation of adipocyte differentiation, which is essential in the early stages of this process [16,29].

To date, only a few studies have shown an association between gap junction communication and differentiation, focusing primarily on myoblasts, osteoblasts and keratinocytes [8–11]. For instance, Balogh et al. [8] showed that a decrease in Cx43 expression was correlated with rat L6 myoblast differentiation. Likewise, Lecanda et al. [9] demonstrated that Cx43 modulates the expression of specific osteoblastic gene products by regulating the transcriptional activity of their promoters. The fact that adipocytes, myoblasts and osteoblasts differentiate from a common mesenchymal progenitor cell [30] suggests that gap junction communication via Cx43 expression and/or phosphorylation could have a vital role during adipocyte differentiation. Indeed, several studies have confirmed there exists a relationship between Cx43 and adipogenesis [15,16]. Yanagiya et al. [16] established that an increase in Cx43 and gap junction communication is required for mitotic clonal expansion during

adipogenesis by showing that 3T3-L1 preadipocytes fail to differentiate in the presence of the gap junction inhibitor 18-α glycyrrhetinic acid (AGA).

The phosphorylation state of Cx43 is a critical determinant of gap junction function [29,31,32]. Cx43 can be phosphorylated at several residues, thus giving rise to multiple electrophoretic species on SDS-polyacrylamide gels [29]. These modifications are linked to the regulation of and by Cx43, likely by influencing the subcellular localization of Cx43, which is a key element in the formation of functional gap junctions. Ours are the first results to show that the subcellular localization of Cx43 also changes in 3T3-L1 as differentiation proceeds, and that its intracellular movement is closely linked to phosphorylation state. While it can be argued that the phosphorylated forms of Cx43 are present on plasma membrane as gap junction channels, we did not confirm that active junctions were formed. Regardless, loss of Cx43 from the plasma membrane by day 4 indicates Cx43 is no longer capable of influencing cell–cell communication since it is no longer present within gap junctions. These findings are in agreement with Azarnia and Russell [14] who showed that adipocytes do not communicate via gap junctions. However, it has also been noted that Cx43 can influence gene expression via a gap junction-independent process [33].

Yanagiya et al. [16] showed that Cx43 expression is required for initiating differentiation (although expression rates are higher on day 7 when Cx43 protein levels are low relative to day 0), but whether down-regulation of Cx43 is also a necessary event had not been tested. Inhibition of proteoasome activity by MG132 treatment resulted in high levels of total Cx43 and inhibition of adipogenesis.

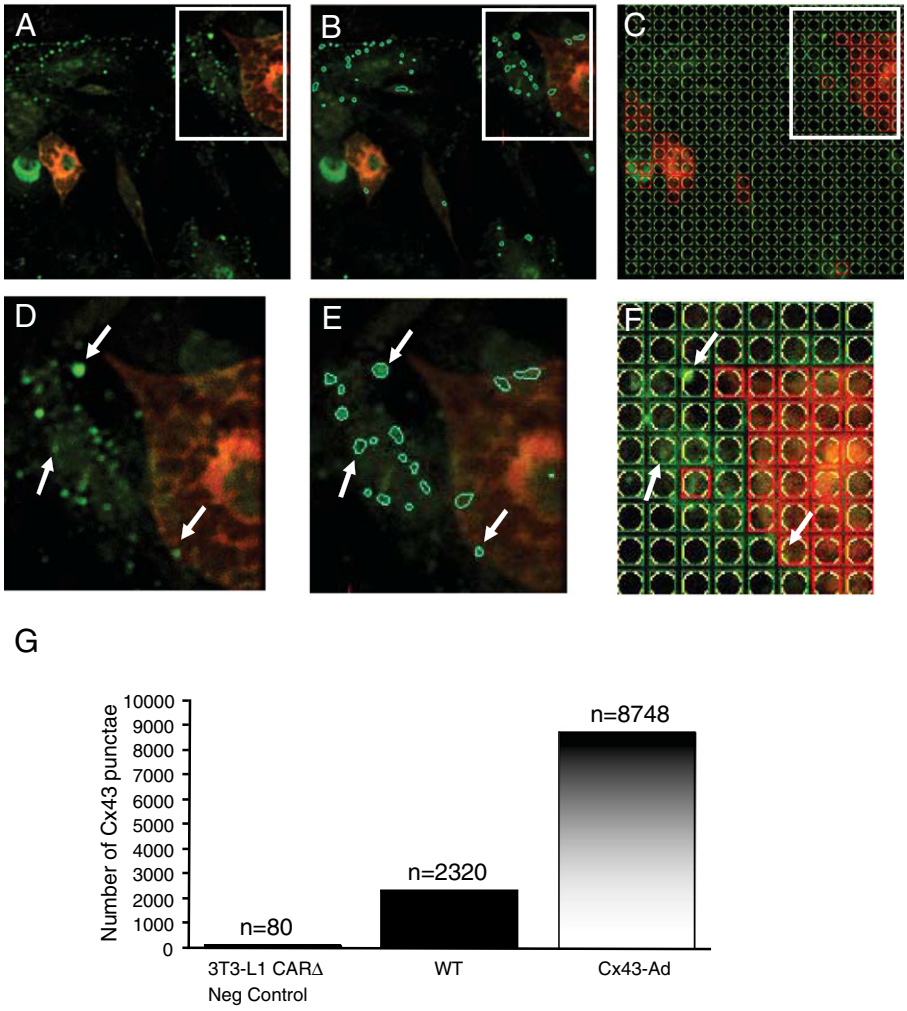

Fig. 7. Laser scanning cytometry (LSC) analysis of Cx43 punctae and FAS expression in wild type and Cx43-adenovirus infected 3T3-L1-CARΔ cells. 3T3-L1-CARΔ cells were infected with Ad5 CMV-Cx43 on day 0 of differentiation. Cells were fixed and co-stained with total Cx43 (green) and FAS (red) and subsequently examined by LSC as described in Materials and methods. (A and D) Micrographs captured using LSC of day 8 3T3-L1-CARΔ cells dual labeled for Cx43 (green) and FAS (red). White box in upper right corner corresponds to area for the zoom image shown in panel (D). Arrows in (D) indicate examples of Cx43 events (punctae) identified using LSC software (see panel E). (B and E) Micrographs showing primary contours generated by LSC software for Cx43 punctae (green) for the images shown in (A) and (D), respectively. Arrows in (E) indicate examples of Cx43 events (punctae) identified using LSC software—individual Cx43 events are outlined by light blue contour lines. White box in upper right corner of (B) corresponds to zoom image shown in panel (E). (C and F) Micrographs showing matrix of circular phantom contours generated by LSC software for measuring cellular FAS (red) expression for the images shown in (A) and (D), respectively. White box in upper right corner of (C) corresponds to zoom image shown in panel (F). In both images circular contours that correspond to FAS negative regions are draw in yellow, whereas contours that correspond to FAS positive regions are drawn using red circles. Arrows in (F) indicate examples of Cx43 events (punctae) identified using LSC software (see panel E). (G) Histogram showing cumulative counts for Cx43 events in uninfected (wild type (WT)) and in day 8 3T3-L1-CARΔ cells infected with Ad5 CMV-Cx43. Cell counts were obtained from multiple scan fields (200×192 μm) with cumulative scan areas from 3.4 to 7 mm^2 in three different samples. Data for 3T3-L1 CARΔ negative (Neg.) control samples correspond to background labeling of wild type cells using fluorochrome-conjugated secondary antibody in the absence of primary antibody. (H) Frequency distribution of FAS fluorescence in phantom contours (events) for uninfected (wild type (WT)) and day 8 3T3-L1-CARΔ cells infected with Ad5 CMV-Cx43. Regions of FAS-positive (+'ve) (shown in red) and FAS negative (−'ve) staining (shown in black) were verified visually using contour maps as show in panel (F). Using LSC software, spatial overlap (association) of independent Cx43 punctae events (see panel E) with FAS −'ve and FAS +'ve regions is also shown in green (overlap with FAS +'ve regions appear in orange). (I) Histogram showing results of the association-analysis completed for Cx43 punctae in Fas −'ve and +'ve regions as shown in panel (H). Data for 3T3-L1 CARΔ negative (Neg) cell counts were obtained from multiple scan fields (200×192 μm) with cumulative scan areas from 3.4 to 7 mm^2 in three different samples.

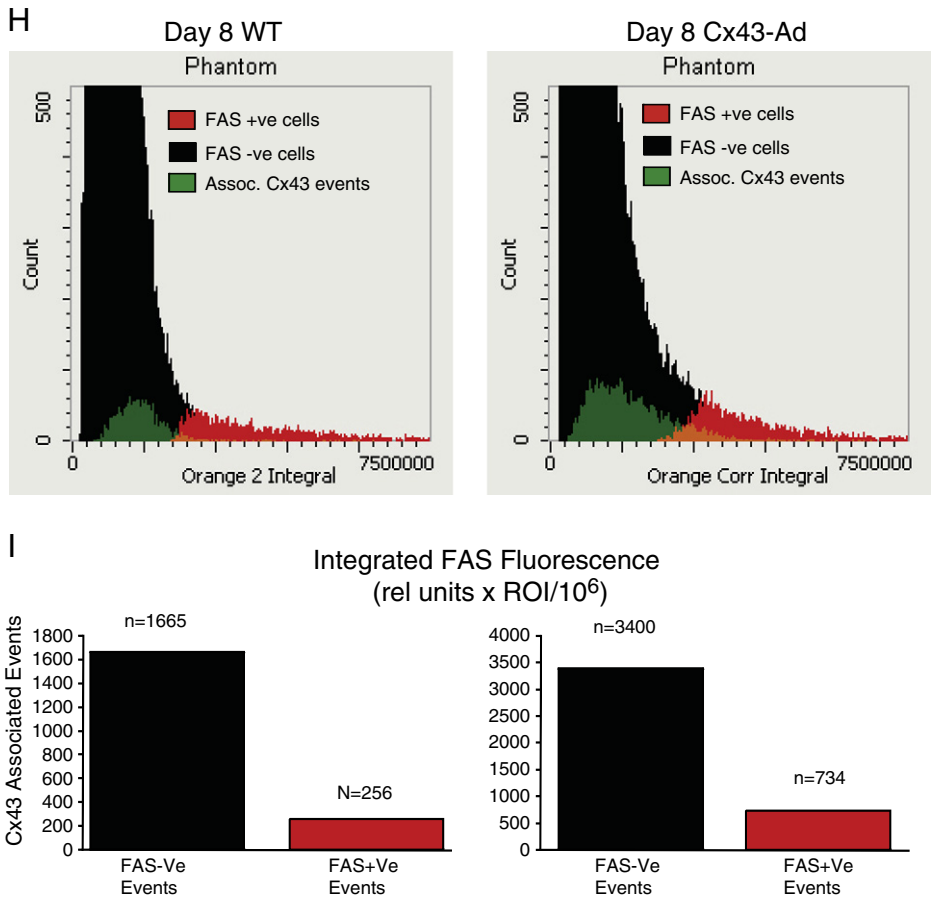

Fig. 7 (*continued*).

In agreement with this finding, constitutive expression of Cx43 during days 4 to 8 of 3T3-L1 CARΔ differentiation via adenoviral infection, the period during which the levels of Cx43 normally decrease, also blocked adipogenesis as indicated by markers of adipocyte maturity and the presence of lipid droplets (Figs. 6 and 7). In both experiments, inhibition of proteasome activity by MG132 and constitutive expression of Cx43 via adenovirus resulted in an increase in phosphorylation of Cx43 as shown in Figs. 5 and 6A, B. These results support the view that the phosphorylation state of Cx43 is a critical factor in adipogenesis. The fact that cells constitutively expressing Cx43 could not effectively differentiate to adipocytes represents the major finding of this investigation. This then leads to the conclusion that down-regulation of Cx43 during adipogenesis is essential for progression to the mature adipocyte. Furthermore, the continued presence of phosphorylated Cx43, whether due to adenoviral expression or as a result of proteasome inhibitor treatment, in conjunction with its presence in the plasma membrane, suggests that functional gap junctions were likely present. Consequently, as shown by Yanagiya et al. [16], it is the presence of active gap junctions that negatively impacts on the differentiation process. Further investigation is therefore warranted to identify the mechanism of Cx43 action on adipocyte differentiation and to examine the relationship between Cx43 phosphorylation, gap junction activity and protein degradation within the context of adipogenesis.

Acknowledgments

Funding for this project was received from the Natural Sciences and Engineering Council of Canada (to PZ) and the Heart and Stroke Foundation of Manitoba (to EK). AJH is supported by the Canada Research Chair Program and received support from the Canada Foundation for Innovation for infrastructure support related to LSC. We would like to thank Nasrin Mesaeli for the antibody to calreticulin, Jeffrey Wigle for providing the adenovirus expressing GFP, Carla Taylor for the Zucker rat adipose tissue and the St. Boniface Hospital Research Foundation for providing the infrastructure that enabled this study.

References

[1] J.C. Saez, V.M. Berthoud, M.C. Branes, A.D. Martinez, E.C. Beyer, Plasma membrane channels formed by connexins: their regulation and functions, Physiol. Rev. 83 (2003) 1359–1400.
[2] A.M. Simon, D.A. Goodenough, D.L. Paul, Mice lacking connexin40 have cardiac conduction abnormalities characteristic of atrioventricular block and bundle branch block, Curr. Biol. 8 (1998) 295–298.
[3] K. Willecke, J. Eiberger, J. Degen, D. Eckardt, A. Romualdi, M. Guldenagel, U. Deutsch, G. Sohl, Structural and functional diversity of connexin genes in the mouse and human genome, Biol. Chem. 383 (2002) 725–737.
[4] P.D. Lampe, A.F. Lau, Regulation of gap junctions by phosphorylation of connexins, Arch. Biochem. Biophys. 384 (2000) 205–215.
[5] L.S. Musil, D.A. Goodenough, Multisubunit assembly of an integral plasma membrane channel protein, gap junction connexin43, occurs after exit from the ER, Cell 74 (1993) 1065–1077.
[6] L.C. Barrio, T. Suchyna, T. Bargiello, L.X. Xu, R.S. Roginski, M.V. Bennett, B.J. Nicholson, Gap junctions formed by connexins 26 and 32 alone and in combination are differently affected by applied voltage, Proc. Natl. Acad. Sci. U. S. A. 88 (1991) 8410–8414.
[7] K. Bittman, D.L. Becker, F. Cicirata, J.G. Parnavelas, Connexin expression in homotypic and heterotypic cell coupling in the developing cerebral cortex, J. Comp. Neurol. 443 (2002) 201–212.
[8] S. Balogh, C.C. Naus, P.A. Merrifield, Expression of gap junctions in cultured rat L6 cells during myogenesis, Dev. Biol. 155 (1993) 351–360.
[9] F. Lecanda, D.A. Towler, K. Ziambaras, S.L. Cheng, M. Koval, T.H. Steinberg, R. Civitelli, Gap junctional communication modulates gene expression in osteoblastic cells, Mol. Biol. Cell 9 (1998) 2249–2258.

[10] P.C. Schiller, G. D'Ippolito, W. Balkan, B.A. Roos, G.A. Howard, Gap-junctional communication is required for the maturation process of osteoblastic cells in culture, Bone 28 (2001) 362–369.
[11] H. Schmalbruch, Skeletal muscle fibers of newborn rats are coupled by gap junctions, Dev. Biol. 91 (1982) 485–490.
[12] P. Cornelius, O.A. MacDougald, M.D. Lane, Regulation of adipocyte development, Annu. Rev. Nutr. 14 (1994) 99–129.
[13] A.K. Student, R.Y. Hsu, M.D. Lane, Induction of fatty acid synthetase synthesis in differentiating 3T3-L1 preadipocytes, J. Biol. Chem. 255 (1980) 4745–4750.
[14] R. Azarnia, T.R. Russell, Cyclic AMP effects on cell-to-cell junctional membrane permeability during adipocyte differentiation of 3T3-L1 fibroblasts, J. Cell Biol. 100 (1985) 265–269.
[15] A. Umezawa, J. Hata, Expression of gap-junctional protein (connexin 43 or alpha 1 gap junction) is down-regulated at the transcriptional level during adipocyte differentiation of H-1/A marrow stromal cells, Cell Struct. Funct. 17 (1992) 177–184.
[16] T. Yanagiya, A. Tanabe, K. Hotta, Gap-junctional communication is required for mitotic clonal expansion during adipogenesis, Obesity (Silver Spring) 15 (2007) 572–582.
[17] D.A. Goodenough, D.L. Paul, Beyond the gap: functions of unpaired connexon channels, Nat. Rev. Mol. Cell Biol. 4 (2003) 285–294.
[18] C.V. Dowling-Warriner, J.E. Trosko, Induction of gap junctional intercellular communication, connexin43 expression, and subsequent differentiation in human fetal neuronal cells by stimulation of the cyclic AMP pathway, Neuroscience 95 (2000) 859–868.
[19] D.J. Orlicky, J. DeGregori, J. Schaack, Construction of stable coxsackievirus and adenovirus receptor-expressing 3T3-L1 cells, J. Lipid Res. 42 (2001) 910–915.
[20] L. Yau, B. Litchie, S. Thomas, B. Storie, N. Yurkova, P. Zahradka, Endogenous mono-ADP-ribosylation mediates smooth muscle cell proliferation and migration via protein kinase N-dependent induction of c-fos expression, Eur. J. Biochem. 270 (2003) 101–110.
[21] W. Srisakuldee, M.M. Jeyaraman, B.E. Nickel, S. Tanguy, Z.S. Jiang, E. Kardami, Phosphorylation of connexin-43 at serine 262 promotes a cardiac injury-resistant state, Cardiovasc. Res. 83 (2009) 672–681.
[22] B.W. Doble, X. Dang, P. Ping, R.R. Fandrich, B.E. Nickel, Y. Jin, P.A. Cattini, E. Kardami, Phosphorylation of serine 262 in the gap junction protein connexin-43 regulates DNA synthesis in cell–cell contact forming cardiomyocytes, J. Cell Sci. 117 (2004) 507–514.
[23] S. Jalali, M. Aghasi, B. Yeganeh, N. Mesaeli, Calreticulin regulates insulin receptor expression and its downstream PI3 Kinase/Akt signalling pathway, Biochim. Biophys. Acta 1783 (2008) 2344–2351.
[24] B.C. Reed, M.D. Lane, Insulin receptor synthesis and turnover in differentiating 3T3-L1 preadipocytes, Proc. Natl. Acad. Sci. U. S. A. 77 (1980) 285–289.
[25] S. De Barros, A. Zakaroff-Girard, M. Lafontan, J. Galitzky, V. Bourlier, Inhibition of human preadipocyte proteasomal activity by HIV protease inhibitors or specific inhibitor lactacystin leads to a defect in adipogenesis, which involves matrix metalloproteinase-9, J. Pharmacol. Exp. Ther. 320 (2007) 291–299.
[26] K. Sakamoto, Y. Sato, M. Sei, A.A. Ewis, Y. Nakahori, Proteasome activity correlates with male BMI and contributes to the differentiation of adipocyte in hADSC, Endocrine 37 (2010) 274–279.
[27] D.J. Orlicky, J. Schaack, Adenovirus transduction of 3T3-L1 cells, J. Lipid Res. 42 (2001) 460–466.
[28] H. Reinecke, E. Minami, J.I. Virag, C.E. Murry, Gene transfer of connexin43 into skeletal muscle, Hum. Gene Ther. 15 (2004) 627–636.
[29] J.L. Solan, P.D. Lampe, Connexin43 phosphorylation: structural changes and biological effects, Biochem. J. 419 (2009) 261–272.
[30] M. Owen, Marrow stromal stem cells, J. Cell Sci. Suppl. 10 (1988) 63–76.
[31] R.G. Johnson, J.K. Reynhout, E.M. TenBroek, B.J. Quade, T. Yasumura, K.G. Davidson, J.D. Sheridan, J.E. Rash, Gap junction assembly: roles for the formation plaque and regulation by the C-terminus of connexin43, Mol. Biol. Cell 23 (2012) 71–86.
[32] J.L. Solan, P.D. Lampe, Connexin phosphorylation as a regulatory event linked to gap junction channel assembly, Biochim. Biophys. Acta 1711 (2005) 154–163.
[33] E. Kardami, X. Dang, D.A. Iacobas, B.E. Nickel, M. Jeyaraman, W. Srisakuldee, J. Makazan, S. Tanguy, D.C. Spray, The role of connexins in controlling cell growth and gene expression, Prog. Biophys. Mol. Biol. 94 (2007) 245–264.